Uncertainty Law in Ambient Modal Identification
Part I: Theory

Siu-Kui Au[*]

Center for Engineering Dynamics and Institute for Risk and Uncertainty

University of Liverpool

Abstract

Ambient vibration test has gained increasing popularity in practice as it provides an economical means for modal identification without artificial loading. Since the signal-to-noise ratio cannot be directly controlled, the uncertainty associated with the identified modal parameters is a primary concern. From a scientific point of view, it is of interest to know what factors the uncertainty depends on and what the relationship is. For planning or specification purposes, it is desirable to have an assessment of the test configuration required to achieve a specified accuracy in the modal parameters. E.g., what is the minimum data duration to achieve a 30% coefficient of variation (c.o.v.) in the damping ratio? To address these questions, this work investigates the leading order behavior of the 'posterior uncertainties' (i.e., given data) of the modal parameters in a Bayesian identification framework. In the context of well-separated modes, small damping and sufficient data, it is shown rigorously that, among other results, the posterior c.o.v. of the natural frequency and damping ratio are asymptotically equal to $(\zeta / 2\pi N_c B_f)^{1/2}$ and $1/(2\pi\zeta N_c B_\zeta)^{1/2}$, respectively; where ζ is the damping ratio; N_c is the data length as a multiple of the natural period; B_f and B_ζ are data length factors that depend only on the bandwidth utilized for identification, for which explicit expressions have been derived. As the Bayesian approach allows full use of information contained in the data, the results are fundamental characteristics of the ambient modal identification problem. This paper develops the main theory. The companion paper investigates the implication of the results and verification with field test data.

[*] Corresponding author. E-mail: siukuiau@liverpool.ac.uk. Office phone: +44 (0)151 794 5217. Formerly City University of Hong Kong.

1. Introduction

The modal properties of a structure primarily include the natural frequencies, damping ratios and mode shapes. Identifying them based on measured vibration data is an important task often performed in vibration control or structural health monitoring [1][2][3][4]. Ambient vibration (output-only) tests have gained increasing popularity in both theory development and practical applications [5][6][7][8]. This is to a large extent attributed to its economy in implementation. Ambient vibration data are obtained when the structure is under unknown working load assumed to be random with broadband spectral characteristics. The latter assumptions are required to establish a theoretical stochastic description of the response statistics without knowing the loading time history.

In ambient vibration tests the loading comes from the stochastic environment whose intensity and frequency content cannot be directly controlled. In the absence of specific loading information, the uncertainty of the identified modal parameters is often significantly larger than that using forced vibration (known input) or free vibration tests where the signal-to-noise (s/n) ratio can be managed to an adequate level. The identified damping ratio, for example, exhibits large variability from one data set to another. The observed variability may come from physical variability, e.g., as a result of thermal or amplitude dependence, or merely statistical variability due to lack of data or modeling error [9][10][11][12][13]. Significant variability can also exist in the mode shape at where the value is small or when the modes are closely-spaced.

It will be useful to assess beforehand the uncertainty in the identified modal properties for given test configuration, although this task can be challenging, recognizing the sophistication of ambient modal identification (operational modal analysis) theories. A Bayesian identification approach allows the 'posterior uncertainty' (i.e., given data) to be calculated for given data and modeling assumptions [14][15][16][17]. However, the expressions depend implicitly on the data and they are too generic to give any insights.

This work investigates the leading order behavior of the posterior uncertainties of modal properties identified using ambient vibration data, with the aim to providing insights for managing their uncertainties. A Bayesian FFT approach is adopted that rigorously processes the information available in the data to yield information about the modal parameters. Working in the frequency domain allows a natural extraction of information in the data relevant to the mode and is well suited to time-invariant linear systems with classical modes. This does not introduce any loss of generality by virtue of the one-one correspondence between the time-domain and FFT data. The original formulation first appeared in [18]. Fast equivalent formulations that allow practical implementations are due to [19][8][20]. A recent review can be found in [21].

To keep the problem tractable we focus on the case of well-separated modes, where one can select a frequency band around the natural frequency of interest so that the contribution of response from other modes can be ignored in the identification model. We analyze in detail the posterior covariance matrix of modal parameters and derive its leading order behavior under asymptotic conditions applicable in typical situations, namely, small damping and long data duration. The outcomes are 'asymptotic uncertainty laws' that govern the achievable limits in the accuracy of modal parameters given the modeling assumptions. This paper develops the theory. The companion paper discusses their qualitative aspects, implications and verification with field data.

2. Bayesian modal identification theory

Let the acceleration time history measured at n degrees of freedom (dofs) of a structure be $\{\hat{\ddot{\mathbf{x}}}_j \in R^n : j = 1,...,N\}$ and abbreviated as $\{\hat{\ddot{\mathbf{x}}}_j\}$, where N is the number of samples per channel. In the context of Bayesian inference, it is modeled as $\hat{\ddot{\mathbf{x}}}_j = \ddot{\mathbf{x}}_j(\boldsymbol{\theta}) + \boldsymbol{\varepsilon}_j$, where $\ddot{\mathbf{x}}_j(\boldsymbol{\theta})$ is the model (theoretical) response that depends on the set of parameters $\boldsymbol{\theta}$ to be identified; $\boldsymbol{\varepsilon}_j$ is the prediction error that accounts for the difference between the model response and data, due to measurement noise and modeling error. The FFT $\{\mathcal{F}_k\}$ of $\{\hat{\ddot{\mathbf{x}}}_j\}$ is defined as:

$$\mathcal{F}_k = \sqrt{\frac{2\Delta t}{N}} \sum_{j=1}^{N} \hat{\ddot{\mathbf{x}}}_j \exp[-2\pi\mathbf{i}\frac{(k-1)(j-1)}{N}] \tag{1}$$

where $\mathbf{i}^2 = -1$ and Δt is the sampling interval. For $k = 2,...,N_q$, $\mathcal{F}_k$ corresponds to frequency $f_k = (k-1)/N\Delta t$, where $N_q = \text{int}[N/2]+1$ ($\text{int}[.]$ denotes the integer part) is the index at the Nyquist frequency. In practice, only the $\mathcal{F}_k$'s on a selected frequency band containing the mode(s) of interest is used for identification, which significantly simplifies the identification model. The power spectral density (PSD) of the loading and prediction error need only be flat within the band. This relaxes the conventional white noise assumption, making the method more robust than time-domain methods. Other bands with irrelevant information or which are difficult to model are legitimately ignored, therefore avoiding modeling error. This does not require any signal pre-processing such as filtering or averaging.

Let the structure be classically-damped, i.e., its response can be written as a sum of modal responses that satisfy their own (uncoupled) equation of motion. Assuming a single contributing mode in the selected band, the FFT of the acceleration response in the band is given by $\mathcal{F}_{\ddot{\mathbf{x}}}(k) = \mathbf{\Phi}\mathcal{F}_{\ddot{\eta}}(k)$ where $\mathbf{\Phi} \in R^n$ is the mode shape confined to the measured dofs assumed to have unit norm, i.e., $\| \mathbf{\Phi} \|^2 = \mathbf{\Phi}^T\mathbf{\Phi} = 1$; $\mathcal{F}_{\ddot{\eta}}(k)$ is the FFT of the modal acceleration response $\ddot{\eta}$, which satisfies the modal equation of motion:

$$\ddot{\eta}(t) + 2\zeta\omega\dot{\eta}(t) + \omega^2\eta(t) = p(t) \tag{2}$$

Here $\omega = 2\pi f$; f is the natural frequency (in Hz), ζ is the damping ratio and $p(t)$ is the modal force (including the modal mass in its denominator) with PSD S within the selected band (i.e., need not be white). The set of parameters $\mathbf{\theta}$ to be identified is then given by

$$\mathbf{\theta} = \{f, \zeta, S, S_e, \mathbf{\Phi}\} \tag{3}$$

where S_e is the PSD of the prediction error within the selected band (i.e., need not be white).

Let $\mathbf{Z}_k = [\mathbf{F}_k ; \mathbf{G}_k] \in R^{2n}$, where $\mathbf{F}_k = \operatorname{Re} \mathcal{F}_k$ and $\mathbf{G}_k = \operatorname{Im} \mathcal{F}_k$. The FFT data within the selected band is denoted by $\{\mathbf{Z}_k\}$. Using Bayes' Theorem, the posterior probability density function (PDF) of the set of modal parameters $\boldsymbol{\theta}$ given the FFT data $\{\mathbf{Z}_k\}$ is given by

$$p(\boldsymbol{\theta} \,|\, \{\mathbf{Z}_k\}) = p(\{\mathbf{Z}_k\} \,|\, \boldsymbol{\theta}) \frac{p(\boldsymbol{\theta})}{p(\{\mathbf{Z}_k\})} \tag{4}$$

This equation turns around the question about the likelihood of $\boldsymbol{\theta}$ given the information of the data $\{\mathbf{Z}_k\}$ into a question about the likelihood of obtaining the data for a given $\boldsymbol{\theta}$. The term $p(\{\mathbf{Z}_k\} \,|\, \boldsymbol{\theta})$ is called the 'likelihood function'. It links the measured data with the identification model and must be constructed based on modeling assumptions. The term $p(\{\mathbf{Z}_k\})$ does not depend on $\boldsymbol{\theta}$ and so it does not affect the posterior PDF. The term $p(\boldsymbol{\theta})$ is called the 'prior PDF', which reflects one's knowledge about $\boldsymbol{\theta}$ in the absence of data. In modal identification, prior information is of little relevance because with sufficient data in practice the variation of the posterior PDF is dominated by that of the likelihood function. Thus, assuming a flat (i.e., constant) prior PDF, the posterior PDF is simply proportional to the likelihood function.

As a standard result in signal processing, for a stationary (or even some weakly non-stationary) stochastic process (possibly vector-valued), the $\mathcal{F}_k$'s at different frequencies (i.e., k) are for large N asymptotically independent and jointly Gaussian [22]. In addition, with a single contributing mode $\mathbf{F}_k$ and $\mathbf{G}_k$ are asymptotically independent. As a result,

$$p(\boldsymbol{\theta} \,|\, \{\mathbf{Z}_k\}) \propto p(\{\mathbf{Z}_k\} \,|\, \boldsymbol{\theta}) = (2\pi)^{-nN_f} [\prod_k \det \mathbf{C}_k(\boldsymbol{\theta})]^{-1/2} \exp[-\frac{1}{2} \sum_k \mathbf{Z}_k^T \mathbf{C}_k(\boldsymbol{\theta})^{-1} \mathbf{Z}_k] \tag{5}$$

where the sum and product are over index k in the selected band with N_f terms; $\mathbf{C}_k(\boldsymbol{\theta})$ is the model covariance matrix of $\mathbf{Z}_k$. For small Δt it is given by [19]

$$\mathbf{C}_k = \frac{SD_k}{2} \begin{bmatrix} \boldsymbol{\Phi}\boldsymbol{\Phi}^T & \mathbf{0}_n \\ \mathbf{0}_n & \boldsymbol{\Phi}\boldsymbol{\Phi}^T \end{bmatrix} + \frac{S_e}{2} \mathbf{I}_{2n} \tag{6}$$

where $\mathbf{0}_n \in R^n$ denotes a zero matrix and $\mathbf{I}_n \in R^{2n}$ denotes the identity matrix;

$$D_k(f,\zeta) = [(\beta_k^2 - 1)^2 + (2\zeta\beta_k)^2]^{-1} \tag{7}$$

resembles the dynamic amplification factor, except that the frequency ratio is defined as

$\beta_k = f / f_k$ (rather than f_k / f). For analysis purpose it is convenient to write

$p(\theta \,|\, \{\mathbf{Z}_k\}) \propto \exp[-L(\theta)]$, where

$$L(\theta) = \frac{1}{2}\sum_k \ln \det \mathbf{C}_k(\theta) + \frac{1}{2}\sum_k \mathbf{Z}_k^T \mathbf{C}_k(\theta)^{-1} \mathbf{Z}_k \tag{8}$$

is called the 'negative log-likelihood function' (NLLF). With sufficient data the posterior PDF of θ can be well-approximated by a Gaussian PDF centered at the most probable value (MPV), which is equivalent to a second order approximation of $L(\theta)$ about the MPV [13]. Correspondingly, the posterior covariance matrix is equal to the inverse of the Hessian of $L(\theta)$ evaluated at the MPV. This Hessian is the primary target of analysis in this work.

It should be noted that the 'raw FFTs' $\{\mathcal{F}_k\}$ are used in the likelihood function and hence in the Bayesian modal identification process. There is no need for averaging or any form of signal processing (e.g., Welch averaging). This is one of the major advantages of the Bayesian FFT method that eliminates possible distortion from signal processing artifacts. Making inference directly based on the FFT as data instead of statistical proxies (e.g., the spectral density) also allows full use of information contained in the data within the selected frequency band.

2.1. Fast equivalent formulation

Due to the non-trivial dependence of the NLLF on the modal parameters, the MPV of the modal parameters and the posterior covariance can only be computed numerically for given data. The NLLF in (8) is not conducive to computations because it involves the inverse of $\mathbf{C}_k$ which is close to singular for data with large s/n ratio and whose dimension grows with the number of measured dofs. In view of this, an alternative equivalent form has been recently derived which allows a fast solution [19]:

$$L = -nN_f \ln 2 + (n-1)N_f \ln S_e + \sum_k \ln(SD_k + S_e) + S_e^{-1}(d - \frac{\boldsymbol{\Phi}^T \mathbf{A} \boldsymbol{\Phi}}{\boldsymbol{\Phi}^T \boldsymbol{\Phi}}) \qquad (9)$$

where

$$\mathbf{A} = \sum_k (1 + \frac{S_e}{SD_k})^{-1} \mathbf{D}_k \qquad (10)$$

$$d = \sum_k (\mathbf{F}_k^T \mathbf{F}_k + \mathbf{G}_k^T \mathbf{G}_k) \qquad (11)$$

$$\mathbf{D}_k = \mathbf{F}_k \mathbf{F}_k^T + \mathbf{G}_k \mathbf{G}_k^T \qquad (12)$$

The significance of (9) is that all terms involved are well-conditioned and the mode shape has been isolated into a quadratic form so that its MPV can be determined analytically. This form has allowed an extremely fast procedure for determining the posterior MPV and covariance matrix. It also allows an analytical study of the posterior uncertainty of modal parameters in this work.

3. Outline of results

In the remaining part of this paper, we shall investigate the leading order behavior of the posterior covariance matrix through the Hessian of the NLLF at the MPV. As will be seen, the mathematical derivations are quite lengthy. However, the results are *remarkably simple*. For the ease of reading, here we summarize the context of the problem and outline the results.

1. *Structure*: The damping ratio ζ is assumed to be small.

2. *Data length*: The data duration T_d is assumed to be long compared to the natural period $T = 1/f$. That is,

$$N_c = \frac{T_d}{T} >> 1 \qquad (13)$$

3. *Spectral information*: The selected frequency band is assumed to be symmetrically centered about the resonance peak with a bandwidth of $2\kappa\zeta$, i.e., $f(1 \pm \kappa\zeta)$, where κ is

called the 'bandwidth factor' and is a $O(1)$ constant (often greater than 1). This parameterization takes into account of the fact that the resonance bandwidth is generally $O(\zeta)$. For example, the half-power band is $f(1\pm\zeta)$; the band $f(1\pm6\zeta)$ accounts for 90% of the response variance. The bandwidth factor depends on the selected frequency band, which is a trade-off between modeling error risk and the information used for modal identification. Since the bandwidth is $2\kappa\zeta f$ and the frequency interval is $1/T_d = 1/N_cT$, the number of FFT ordinates in the selected band is equal to

$$N_f = \frac{2\kappa\zeta f}{1/N_cT} = 2\kappa\zeta N_c \tag{14}$$

This is assumed to be large.

In the above context, we will show that the (squared) posterior coefficient of variation (c.o.v.=standard deviation/MPV) of modal parameters are given by, to the leading order,

$$\delta_f^2 \sim \frac{\zeta}{2\pi N_c B_f(\kappa)}, \ \delta_\zeta^2 \sim \frac{1}{2\pi\zeta N_c B_\zeta(\kappa)}, \ \delta_S^2 \sim \frac{1}{N_f B_S(\kappa)}, \ \delta_{S_e}^2 \sim \frac{1}{(n-1)N_f} \tag{15}$$

where

$$B_f(\kappa) = \frac{2}{\pi}(\tan^{-1}\kappa - \frac{\kappa}{\kappa^2+1}), \ B_\zeta(\kappa) = \frac{2}{\pi}\left[\tan^{-1}\kappa + \frac{\kappa}{\kappa^2+1} - \frac{2(\tan^{-1}\kappa)^2}{\kappa}\right]$$

$$B_S(\kappa) = 1 - 2(\tan^{-1}\kappa)^2\kappa^{-1}(\tan^{-1}\kappa + \frac{\kappa}{\kappa^2+1})^{-1} \tag{16}$$

are 'data length factors' that only depend on the bandwidth factor κ.

Assuming that the mode shape is normalized to have unit norm, i.e., $\mathbf{\Phi}^T\mathbf{\Phi} = 1$, its posterior covariance matrix is given by

$$\mathbf{C}_\Phi \sim \frac{\nu\zeta}{N_c B_\Phi(\kappa)}(\mathbf{I}_n - \mathbf{\Phi}\mathbf{\Phi}^T) \tag{17}$$

where

$$B_\Phi(\kappa) = \tan^{-1}\kappa \tag{18}$$

is the bandwidth factor for the mode shape; and

$$v = \frac{S_e}{S} \qquad (19)$$

is called the 'noise-to-environment' (n/e) ratio. The 'expected Modal Assurance Criterion' (MAC) [23] that quantifies the overall uncertainty of the mode shape is given by

$$\bar{\rho} \sim (1 + \delta_\Phi^2)^{-1/2} \qquad (20)$$

where δ_Φ^2 is the sum of principle variances (i.e., eigenvalues) of $\mathbf{C}_\Phi$ given by

$$\delta_\Phi^2 \sim \frac{(n-1)v\zeta}{N_c B_\Phi(\kappa)} \qquad (21)$$

Significant correlation exists only between ζ and S, which is $O(\kappa^{-1/2})$. The correlation between any other pair among $f, \zeta, S, S_e, \mathbf{\Phi}$ is asymptotically small, at most $O(\zeta)$.

Table 1 summarizes these results, which are asymptotically correct as $\zeta \to 0$ and $N_c, N_f \to \infty$. They depend only on the (dimensionless) scales ζ, v, κ and N_c. These 'uncertainty laws' shall be proven in Sections 5 to 7 of this paper, before which the analysis strategy shall be outlined in Section 4. Readers interested in applications may skip to the companion paper, where the implication and verification of the uncertainty laws will be discussed.

4. Analysis strategy and preliminaries

From first glance it seems unlikely that the posterior covariance matrix can be expressed in a simple form because it is the inverse of the Hessian, which is a $(4+n)$-square full matrix with each entry given by a complicated expression implicitly in terms of modal parameters and data. It turns out, however, that significant simplifications can result under the asymptotic conditions. These are outlined logically as follows.

As will be discussed in Sections 4.1 and 4.2, we make use of the fact that the main contribution of the sums in (9) and (10) comes from the resonance region for which

$\beta_k \sim 1$ and $\gamma_k = SD_k / S_e \gg 1$. This allows us to obtain a simpler form for the NLLF and its second derivatives. To study the leading order behavior, when analyzing the Hessian of the NLLF we replace the MPV by the value corresponding to the data and model the latter by a stochastic representation consistent with identification assumptions. This is legitimate because the random deviatory part is of smaller order.

Critical facts have been discovered that significantly simplify analysis of the Hessian. We will show in Section 5 that at the MPV the cross-derivatives of the NLLF with respect to S_e and the remaining parameters are asymptotically small, implying that S_e is 'decoupled' from them. The same is also true for the mode shape $\mathbf{\Phi}$, as will be shown in Section 6. The Hessian then has a block diagonal structure and its inverse is simply a block diagonal matrix containing the inverse of the individual blocks. The decoupling of S_e and $\mathbf{\Phi}$ implies that the covariance matrix of the remaining parameters (f, ζ, S) can be obtained as the inverse of the corresponding 3-by-3 partition in the Hessian. This inverse can be managed algebraically, resulting in close form expressions. This will be shown in Section 7. The remaining part of this section introduces the mathematical facilities that are used for developing the theory.

4.1. Asymptotics of log-likelihood function

The analysis starts with an asymptotic expression for the NLLF for small ζ. Recall the NLLF in (9). For small ζ and $\beta_k \sim 1$, one has $D_k \gg 1$ and

$$\gamma_k = \frac{SD_k}{S_e} \gg 1 \tag{22}$$

Consider the following Taylor expansions for small $\gamma_k^{-1} = S_e / SD_k$:

$$\sum_k \ln(SD_k + S_e) \sim \sum_k \ln SD_k + \sum_k S_e S^{-1} D_k^{-1} - \frac{1}{2} \sum_k S_e^2 S^{-2} D_k^{-2} \tag{23}$$

$$\mathbf{A} = \sum_k (1 + \frac{S_e}{SD_k})^{-1} \mathbf{D}_k \sim \mathbf{A}_0 - S_e S^{-1} \sum_k D_k^{-1} \mathbf{D}_k + S_e^2 S^{-2} \sum_k D_k^{-2} \mathbf{D}_k \tag{24}$$

where

$$\mathbf{A}_0 = \sum_k \mathbf{D}_k \qquad (25)$$

Applying up to the first order of these approximations to (9) and rearranging yields

$$L \sim -nN_f \ln 2 + \sum_k \ln D_k + S_e S^{-1} \sum_k D_k^{-1}$$

$$+ \left[(n-1)N_f \ln S_e + S_e^{-1}(d - \frac{\mathbf{\Phi}^T \mathbf{A}_0 \mathbf{\Phi}}{\mathbf{\Phi}^T \mathbf{\Phi}}) \right] + \left[N_f \ln S + S^{-1} \sum_k D_k^{-1} \frac{\mathbf{\Phi}^T \mathbf{D}_k \mathbf{\Phi}}{\mathbf{\Phi}^T \mathbf{\Phi}} \right] \qquad (26)$$

Without much loss of generality we assume that $n > 1$ so that the term $(n-1)N_f \ln S_e$ in the first bracket of (26) does not vanish. This form leads to the asymptotic MPV for S, S_e and $\mathbf{\Phi}$ [8].

Direct differentiation of (26) and evaluating at the MPV gives the derivatives of the NLLF as follows. For simplicity in notation, we use a variable in the superscripted parenthesis to denote a derivative with respect to it (e.g., $D_k^{(f\zeta)} \equiv \partial^2 D_k / \partial f \partial \zeta$). Also, the MPV is denoted directly by its parameter symbol. The auto-derivatives (evaluated at the MPV) are given by:

$$L^{(ff)} \sim \sum_k (\ln D_k)^{(ff)} + S^{-1} \sum_k (D_k^{-1})^{(ff)} (\mathbf{\Phi}^T \mathbf{D}_k \mathbf{\Phi} + S_e) \qquad (27)$$

$$L^{(\zeta\zeta)} \sim \sum_k (\ln D_k)^{(\zeta\zeta)} + S^{-1} \sum_k (D_k^{-1})^{(\zeta\zeta)} (\mathbf{\Phi}^T \mathbf{D}_k \mathbf{\Phi} + S_e) \qquad (28)$$

$$L^{(SS)} \sim N_f S^{-2} \qquad (29)$$

$$L^{(S_e S_e)} \sim (n-1)N_f S_e^{-2} \qquad (30)$$

$$L^{(\mathbf{\Phi}\mathbf{\Phi})} \sim 2S_e^{-1}(\lambda_0 \mathbf{I}_n - \mathbf{A}_0) \qquad (31)$$

where λ_0 is the largest eigenvalue of $\mathbf{A}_0$. The asymptotic nature of (27) to (31) inherits from (26). The second derivative of the third term $S_e S^{-1} \sum_k D_k^{-1}$ in (26) has been omitted from (29) because it is dominated by the leader order term shown. For the same reason the second derivative of the term $\mathbf{\Phi}^T \mathbf{D}_k \mathbf{\Phi} / \mathbf{\Phi}^T \mathbf{\Phi}$ has been omitted from (31). The cross-derivatives (evaluated at the MPV), on the other hand, are given by:

$$L^{(f\zeta)} \sim \sum_k (\ln D_k)^{(f\zeta)} + S^{-1} \sum_k (D_k^{-1})^{(f\zeta)} (\mathbf{\Phi}^T \mathbf{D}_k \mathbf{\Phi} + S_e) \qquad (32)$$

$$L^{(fS)} \sim -S^{-2} \sum_k (D_k^{-1})^{(f)} (\mathbf{\Phi}^T \mathbf{D}_k \mathbf{\Phi} + S_e) \tag{33}$$

$$L^{(\zeta S)} \sim -S^{-2} \sum_k (D_k^{-1})^{(\zeta)} (\mathbf{\Phi}^T \mathbf{D}_k \mathbf{\Phi} + S_e) \tag{34}$$

$$L^{(fS_e)} \sim S^{-1} \sum_k (D_k^{-1})^{(f)} \tag{35}$$

$$L^{(\zeta S_e)} \sim S^{-1} \sum_k (D_k^{-1})^{(\zeta)} \tag{36}$$

$$L^{(SS_e)} \sim -S^{-2} \sum_k D_k^{-1} \tag{37}$$

$$L^{(S_e \Phi)} \sim \mathbf{0} \tag{38}$$

$$L^{(f\Phi)} \sim 2S^{-1} \sum_k (D_k^{-1})^{(f)} [\mathbf{\Phi}^T \mathbf{D}_k - (\mathbf{\Phi}^T \mathbf{D}_k \mathbf{\Phi}) \mathbf{\Phi}^T] \tag{39}$$

$$L^{(\zeta\Phi)} \sim 2S^{-1} \sum_k (D_k^{-1})^{(\zeta)} [\mathbf{\Phi}^T \mathbf{D}_k - (\mathbf{\Phi}^T \mathbf{D}_k \mathbf{\Phi}) \mathbf{\Phi}^T] \tag{40}$$

$$L^{(S\Phi)} \sim -2S^{-2} \sum_k D_k^{-1} [\mathbf{\Phi}^T \mathbf{D}_k - (\mathbf{\Phi}^T \mathbf{D}_k \mathbf{\Phi}) \mathbf{\Phi}^T] \tag{41}$$

Note that the mode shape $\mathbf{\Phi}$ is assumed to have unit norm, i.e., $\| \mathbf{\Phi} \|^2 = \mathbf{\Phi}^T \mathbf{\Phi} = 1$. The above expressions will be used later for studying their asymptotic behavior. The derivatives of D_k involved in these expressions are given in Appendix I. As the term $\mathbf{\Phi}^T \mathbf{D}_k \mathbf{\Phi}$ appears frequently in the derivatives we analyze its leading order behavior in the next subsection.

4.2. Asymptotics of spectral density matrix

Although the term $\mathbf{\Phi}^T \mathbf{D}_k \mathbf{\Phi}$ depends on the measured data which is unknown prior to testing, it is possible to assess its leading order behavior based on modeling assumptions built in the identification process. Recall from (12) that $\mathbf{D}_k = \mathbf{F}_k \mathbf{F}_k^T + \mathbf{G}_k \mathbf{G}_k^T$. Since $\mathbf{F}_k$ and $\mathbf{G}_k$ are independent and identically distributed (i.i.d.), it is sufficient to investigate the behavior of $\mathbf{F}_k \mathbf{F}_k^T$. Within the selected band, $\mathbf{F}_k$ is dominated by a single mode in combination with the prediction error. It can be represented by

$$\mathbf{F}_k = \sqrt{\frac{SD_k}{2}} X_k \mathbf{\Phi} + \sqrt{\frac{S_e}{2}} \mathbf{W}_k \tag{42}$$

where X_k is a standard Gaussian random variable (i.e., zero mean, unit variance) associated with the FFT of the modal response and $\mathbf{W}_k$ is an n-dimensional standard Gaussian vector with independent components associated with the prediction error; X_k and $\mathbf{W}_k$ are independent. It can be easily checked using (42) that $E[\mathbf{F}_k] = \mathbf{0}$ and $E[\mathbf{F}_k \mathbf{F}_k^T] = (SD_k \boldsymbol{\Phi}\boldsymbol{\Phi}^T + S_e \mathbf{I}_n)/2$. Expanding the terms,

$$\mathbf{F}_k\mathbf{F}_k^T = \frac{SD_k}{2}X_k^2\boldsymbol{\Phi}\boldsymbol{\Phi}^T + \frac{S_e}{2}\mathbf{W}_k\mathbf{W}_k^T + \frac{1}{2}\sqrt{S_e SD_k}X_k(\boldsymbol{\Phi}\mathbf{W}_k^T + \mathbf{W}_k\boldsymbol{\Phi}^T) \tag{43}$$

Summing (43) over k,

$$\sum_k \mathbf{F}_k\mathbf{F}_k^T = \boldsymbol{\Phi}\boldsymbol{\Phi}^T\sum_k \frac{SD_k}{2}X_k^2 + \frac{S_e}{2}\sum_k \mathbf{W}_k\mathbf{W}_k^T + \frac{\sqrt{S_e S}}{2}\sum_k \sqrt{D_k}X_k(\boldsymbol{\Phi}\mathbf{W}_k^T + \mathbf{W}_k\boldsymbol{\Phi}^T) \tag{44}$$

The summand in the first term is a positive scalar. The summand in the second term is a positive definite (random) matrix. Consequently the first two terms are $O(N_f)$. The third term is a sum of uncorrelated matrices with zero mean. It is generally $O(N_f^{1/2})$ and therefore can be neglected compared to the first two terms. Thus, to the leading order,

$$\sum_k \mathbf{F}_k\mathbf{F}_k^T \sim \boldsymbol{\Phi}\boldsymbol{\Phi}^T\sum_k \frac{SD_k}{2}X_k^2 + \frac{S_e}{2}\sum_k \mathbf{W}_k\mathbf{W}_k^T \tag{45}$$

Writing X_k^2 and $\mathbf{W}_k\mathbf{W}_k^T$ as a sum of its mean and a (zero-mean) deviatory part, the sums in (45) can be further separated into a sum of the expectation and a sum of the deviatory parts. The former is $O(N_f)$ while the latter is $O(N_f^{1/2})$ because the deviatory parts are uncorrelated with zero mean. Consequently, for large N_f the expression in (45) is dominated by its expectation, i.e.,

$$\sum_k \mathbf{F}_k\mathbf{F}_k^T \sim \boldsymbol{\Phi}\boldsymbol{\Phi}^T(\sum_k \frac{SD_k}{2}) + \frac{S_e}{2}N_f\mathbf{I}_n \tag{46}$$

As $\sum_k \mathbf{G}_k\mathbf{G}_k^T$ has the same asymptotic behavior,

$$\mathbf{A}_0 \sim \boldsymbol{\Phi}\boldsymbol{\Phi}^T(\sum_k SD_k) + S_e N_f\mathbf{I}_n \tag{47}$$

We next investigate the eigenvalues of $\mathbf{A}_0$. Let $\{\mathbf{a}_j \in R^n : j = 1,...,n\}$ be an orthonormal basis with $\mathbf{a}_1 = \mathbf{\Phi}$. Substituting $\mathbf{I}_n = \sum_{j=1}^{n} \mathbf{a}_j \mathbf{a}_j^T$ into (47) gives

$$\mathbf{A}_0 \sim \mathbf{a}_1 \mathbf{a}_1^T \sum_k (SD_k + S_e) + S_e N_f \sum_{j=2}^{n} \mathbf{a}_j \mathbf{a}_j^T \tag{48}$$

This indicates that asymptotically the largest eigenvalue of $\mathbf{A}_0$ is given by

$$\lambda_0 \sim \sum_k (SD_k + S_e) \tag{49}$$

and the remaining $(n-1)$ eigenvalues of $\mathbf{A}_0$ are all equal to $S_e N_f$. Consequently,

$$\sum_k \mathbf{\Phi}^T \mathbf{D}_k \mathbf{\Phi} = \mathbf{\Phi}^T (\sum_k \mathbf{D}_k) \mathbf{\Phi} = \mathbf{\Phi}^T \mathbf{A}_0 \mathbf{\Phi} = \lambda_0 \sim \sum_k (SD_k + S_e) \tag{50}$$

4.3. Decoupling

Significant simplification results by discovering that the prediction error S_e and the mode shape $\mathbf{\Phi}$ are asymptotically 'decoupled' from the remaining parameters. This shall be investigated in the next section. For this purpose we introduce a working definition for 'decoupling'. A parameter θ_i is 'perfectly decoupled' from the remaining ones if (at the MPV) $L^{(\theta_i \theta_j)} = 0$ for all $j \neq i$. In general, the coupling of a scalar-valued parameter with the remaining ones can be considered small if $|q_{\theta_i \theta_j}| \ll 1$ for all $j \neq i$, where

$$q_{\theta_i \theta_j} = \frac{L^{(\theta_i \theta_j)}}{[L^{(\theta_i \theta_i)}]^{1/2} [L^{(\theta_j \theta_j)}]^{1/2}} \tag{51}$$

is a dimensionless 'cross-sensitivity coefficient' between θ_i and θ_j. This idea can be extended to assessing the decoupling of the mode shape $\mathbf{\Phi}$, which is vector-valued. In this case, the sensitivity coefficient is defined as

$$q_{\theta_j \Phi} = \max_{\substack{\mathbf{u} \in R^n \\ \|\mathbf{u}\|=1}} \frac{L^{(\theta_j \Phi)} \mathbf{u}}{[L^{(\theta_j \theta_j)}]^{1/2} [\mathbf{u}^T L^{(\Phi\Phi)} \mathbf{u}]^{1/2}} \tag{52}$$

The mathematical basis of this definition is as follows. Consider the second order Taylor series of the NLLF subjected to small increments $\Delta\theta_j$ and $\Delta\mathbf{\Phi}$ about the MPV:

$$\Delta L = L(\theta_j + \Delta\theta_j, \boldsymbol{\Phi} + \Delta\boldsymbol{\Phi}) - L(\theta_j, \boldsymbol{\Phi}) \approx \frac{1}{2}(Q_{\theta_j\theta_j} + 2Q_{\theta_j\Phi} + Q_{\Phi\Phi}) \tag{53}$$

where the first order terms vanish due to optimality; and

$$Q_{\theta_j\theta_j} = L^{(\theta_j\theta_j)}\Delta\theta_j^2, \ Q_{\theta_j\Phi} = \Delta\theta_j L^{(\theta_j\Phi)}\Delta\boldsymbol{\Phi}, \ Q_{\Phi\Phi} = \Delta\boldsymbol{\Phi}^T L^{(\Phi\Phi)}\Delta\boldsymbol{\Phi} \tag{54}$$

Writing (53) in complete-square form,

$$\Delta L \approx \frac{1}{2}(Q_{\theta_j\theta_j}^{1/2} + Q_{\Phi\Phi}^{1/2})^2 - Q_{\theta_j\theta_j}^{1/2}Q_{\Phi\Phi}^{1/2}(1-q) \tag{55}$$

where $q = Q_{\theta_j\Phi}/Q_{\theta_j\theta_j}^{1/2}Q_{\Phi\Phi}^{1/2}$. Using (54) and writing $\Delta\boldsymbol{\Phi} = \|\Delta\boldsymbol{\Phi}\|\mathbf{u}$, where $\mathbf{u} \in R^n$ is a unit

vector, we have $q = L^{(\theta_j\Phi)}\mathbf{u}/[L^{(\theta_j\theta_j)}]^{1/2}[\mathbf{u}^T L^{(\Phi\Phi)}\mathbf{u}]^{1/2}$. Thus, if $|q| \ll 1$ for any unit vector $\mathbf{u}$

then the second term in (55) is approximately $Q_{\theta_j\theta_j}^{1/2}Q_{\Phi\Phi}^{1/2}$ and hence $\Delta L \approx (Q_{\theta_j\theta_j}^2 + Q_{\Phi\Phi}^2)/2$,

which does not involve any cross derivative term between θ_j and $\boldsymbol{\Phi}$. This condition is

equivalent to $|q_{\theta_j\Phi}| \ll 1$ defined in (52). Table 2 gives a summary of the sensitivity

coefficients in terms of their scaling order, which will be derived later in the paper.

5. Uncertainty law for prediction error PSD

5.1. Decoupling

We show here that S_e is asymptotically decoupled from the remaining parameters, i.e.,

q_{fS_e}, $q_{\zeta S_e}$, q_{SS_e} and $q_{S_e\Phi}$ are asymptotically small compared to 1. First, consider q_{fS_e}.

Substituting (109) from Appendix I into (35) gives,

$$L^{(fS_e)} \sim 4S^{-1}f^{-1}\sum_k \beta_k^2(\beta_k^2 - 1 + 2\zeta^2) = 4S^{-1}f^{-1}\left[\sum_k \beta_k^2(\beta_k + 1)(\beta_k - 1) + 2\zeta^2\sum_k \beta_k^2\right] \tag{56}$$

Taking $\beta_k \sim 1$ and simplifying,

$$L^{(fS_e)} \sim 8S^{-1}f^{-1}[\zeta^2 N_f + \sum_k (\beta_k - 1)] \tag{57}$$

The magnitude of the sum can be assessed using (125) from Appendix II with $a = 0$ and

$b = 1$ (first case), giving $\sum_k (\beta_k - 1) = O(\kappa^3\zeta^3 N_c)$. This implies that, since

$$\zeta^2 N_f = O(\kappa\zeta^3 N_c),$$

$$L^{(fS_e)} = O(S^{-1}f^{-1}\kappa^3\zeta^3 N_c) \tag{58}$$

On the other hand, from (30), $L^{(S_e S_e)} = O(N_f S_e^{-2} n) = O(S_e^{-2}\kappa\zeta n N_c)$. It is shown later (see

(94)) that $L^{(ff)} = O(f^{-2}\zeta^{-1}N_c)$. Combining these orders and noting $v = S_e / S$ gives

$$q_{fS_e} = O(v\kappa^{5/2}\zeta^3 n^{-1/2}) << 1 \tag{59}$$

We next consider $q_{\zeta S_e}$. Substituting (110) from Appendix I into (36) gives, taking $\beta_k \sim 1$,

$$L^{(\zeta S_e)} \sim 8S^{-1}\zeta\sum_k \beta_k^2 \sim 8S^{-1}\zeta N_f = 16S^{-1}\kappa\zeta^2 N_c = O(S^{-1}\kappa\zeta^2 N_c) \tag{60}$$

From (135) of Appendix IV, $L^{(\zeta\zeta)} = O(\zeta^{-1}N_c)$. Combining these orders gives

$$q_{\zeta S_e} = O(v\kappa^{1/2}\zeta^2 n^{-1/2}) << 1 \tag{61}$$

For q_{SS_e}, recall from (37) that $L^{(SS_e)} = -S^{-2}\sum_k D_k^{-1}$. Using (124) from Appendix II with

$a = -1$ and $b = 0$ (first case) gives $\sum_k D_k^{-1} = O(\kappa^3\zeta^3 N_c)$ and hence

$L^{(SS_e)} = O(S^{-2}\kappa^3\zeta^3 N_c)$. From (29), $L^{(SS)} \sim S^{-2}N_f = O(S^{-2}\kappa\zeta N_c)$. Combining these orders

gives

$$q_{SS_e} = O(v\kappa^2\zeta^2 n^{-1/2}) << 1 \tag{62}$$

For $L^{(S_e\Phi)}$, the form in (26) gives $L^{(S_e\Phi)} \sim \mathbf{0}$ in (38) because asymptotically $\mathbf{\Phi}$ is the

eigenvector of $\mathbf{A}_0$. To determine the leading order, we need to consider the second order

term in (24) that has been omitted from (26). This gives a term of

$-S_e S^{-2}\sum_k D_k^{-2}\mathbf{\Phi}^T\mathbf{D}_k\mathbf{\Phi}/\mathbf{\Phi}^T\mathbf{\Phi}$ in the expression of L. Differentiating with respect to S_e

and $\mathbf{\Phi}$, and evaluating at the MPV gives

$$L^{(S_e\Phi)} \sim -2S^{-2}\sum_k D_k^{-2}[\mathbf{\Phi}^T\mathbf{D}_k - (\mathbf{\Phi}^T\mathbf{D}_k\mathbf{\Phi})\mathbf{\Phi}^T] \tag{63}$$

Using this form it is shown in (164) of Appendix IV that for any unit vector $\mathbf{u} \in R^n$,

$$L^{(S_e\Phi)}\mathbf{u} = O(v^{3/2}S_e^{-1}\kappa^{7/2}\zeta^{7/2}N_c^{1/2}) \tag{64}$$

Combining with $L^{(S_e S_e)} = O(S_e^{-2}\kappa\zeta n N_c)$ (see (30)) and $\mathbf{u}^T L^{(\Phi\Phi)}\mathbf{u} = O(v^{-1}\zeta^{-1}N_c)$ (see (85)

later),

$$q_{S_e\Phi} = O(\nu^2\kappa^3\zeta^{7/2}n^{-1/2}N_c^{-1/2}) \ll 1 \tag{65}$$

In summary, q_{fS_e}, $q_{\zeta S_e}$, q_{SS_e} and $q_{S_e\Phi}$ are all asymptotically small, and so S_e is asymptotically decoupled from the remaining parameters.

5.2. Posterior variance

Since S_e is decoupled from the remaining parameters, its posterior variance is simply equal to the reciprocal of $L^{(S_eS_e)}$, i.e.,

$$\text{var}[S_e] = L^{(S_eS_e)^{-1}} \sim S_e^2(n-1)^{-1}N_f^{-1} \tag{66}$$

The (squared) coefficient of variation of S_e is given by

$$\delta_{S_e}^2 = (n-1)^{-1}N_f^{-1} \tag{67}$$

This result assumes that $n > 1$, for otherwise the term involving $\ln S_e$ in (26) vanishes and other terms will dominate.

6. Uncertainty law for mode shape

6.1. Decoupling

We show that, similar to S_e, Φ is also asymptotically decoupled from the remaining parameters, i.e., $q_{f\Phi}$, $q_{\zeta\Phi}$, $q_{S\Phi}$ and $q_{S_e\Phi}$ are all small compared to unity. Since Φ is vector-valued, the cross-sensitivity coefficient is defined by (52).

We first analyze the leading order behavior of $q_{f\Phi}$, which involves studying the magnitude of $L^{(f\Phi)}\mathbf{u}$ for any unit vector $\mathbf{u} \in R^n$. The latter can be interpreted as the projection of $L^{(f\Phi)}$ along the direction of $\mathbf{u}$. We shall first study the projection of $L^{(f\Phi)}$ on an orthonormal basis. From this, the projection on $\mathbf{u}$ can be established, since any $\mathbf{u}$ can be represented as a linear combination of the basis vectors.

Recall $L^{(f\Phi)}$ from (39). Let $\{\mathbf{a}_j \in R^n : j = 1,...,n\}$ be an orthonormal basis with $\mathbf{a}_1 = \Phi$.

For $j = 2,...,n$, since $\Phi^T \mathbf{a}_j = 0$ by orthogonality,

$$L^{(f\Phi)}\mathbf{a}_j \sim 2S^{-1}\sum_k (D_k^{-1})^{(f)}\Phi^T \mathbf{D}_k \mathbf{a}_j = 2S^{-1}\sum_k (D_k^{-1})^{(f)}(\Phi^T \mathbf{F}_k \mathbf{F}_k^T \mathbf{a}_j + \Phi^T \mathbf{G}_k \mathbf{G}_k^T \mathbf{a}_j) \tag{68}$$

Using (43) and simplifying gives

$$\Phi^T \mathbf{F}_k \mathbf{F}_k^T \mathbf{a}_j = \frac{S_e}{2}(\mathbf{W}_k^T \mathbf{a}_j)(\Phi^T \mathbf{W}_k + \gamma_k^{1/2} X_k) \tag{69}$$

Note that $\gamma_k^{1/2} X_k = O(\gamma_k^{1/2})$. Since Φ is a unit vector and $\mathbf{W}_k$ is a standard Gaussian vector with uncorrelated components, $\Phi^T \mathbf{W}_k$ is a sum of uncorrelated random variables and it has zero mean and unit variance. This means that $\Phi^T \mathbf{W}_k = O(1) << \gamma_k^{1/2}$ and therefore

$$\Phi^T \mathbf{F}_k \mathbf{F}_k^T \mathbf{a}_j \sim \frac{1}{2}S_e\gamma_k^{1/2}(\mathbf{W}_k^T \mathbf{a}_j)X_k \qquad\qquad j = 2,...,n \tag{70}$$

Using this result and substituting (109) from Appendix I for $(D_k^{-1})^{(f)}$ gives

$$2S^{-1}\sum_k (D_k^{-1})^{(f)}\Phi^T \mathbf{F}_k \mathbf{F}_k^T \mathbf{a}_j \sim 4S_e S^{-1}f^{-1}\sum_k \beta_k^2(\beta_k^2 - 1 + 2\zeta^2)\gamma_k^{1/2}(\mathbf{W}_k^T \mathbf{a}_j)X_k \tag{71}$$

This is a sum of uncorrelated random variables with zero mean, whose magnitude can be assessed by its standard deviation. The variance of the sum is equal to the sum of the individual variances, giving

$$\mathrm{var}[2S^{-1}\sum_k (D_k^{-1})^{(f)}\Phi^T \mathbf{F}_k \mathbf{F}_k^T \mathbf{a}_j] \sim 16S_e S^{-1}f^{-2}\sum_k \beta_k^4(\beta_k^2 - 1 + 2\zeta^2)^2 D_k \tag{72}$$

since $\gamma_k = SD_k / S_e$ and

$$\mathrm{var}[(\mathbf{W}_k^T \mathbf{a}_j)X_k] = E[(\mathbf{W}_k^T \mathbf{a}_j)^2 X_k^2] = E[(\mathbf{W}_k^T \mathbf{a}_j)^2]E[X_k^2] = 1 \tag{73}$$

Using $v = S_e / S$ and $\beta_k^4(\beta_k^2 - 1 + 2\zeta^2)^2 \sim 4(\beta_k - 1)^2$,

$$\mathrm{var}[2S^{-1}\sum_k (D_k^{-1})^{(f)}\Phi^T \mathbf{F}_k \mathbf{F}_k^T \mathbf{a}_j] \sim 64f^{-2}v\sum_k D_k(\beta_k - 1)^2 \tag{74}$$

Applying (124) from Appendix II with $a = 1$ and $b = 2$ (first case), $\sum_k D_k(\beta_k - 1)^2 = O(\kappa\zeta N_c)$ and so

$$\mathrm{var}[2S^{-1}\sum_k (D_k^{-1})^{(f)}\Phi^T \mathbf{F}_k \mathbf{F}_k^T \mathbf{a}_j] = O(f^{-2}v\kappa\zeta N_c) \tag{75}$$

Since $\mathbf{G}_k$ has the same behavior as $\mathbf{F}_k$, we obtain

$$L^{(f\Phi)}\mathbf{a}_j = O(f^{-1}v^{1/2}\kappa^{1/2}\zeta^{1/2}N_c^{1/2}) \qquad j=2,3,...,n \tag{76}$$

Note also that $L^{(f\Phi)}\mathbf{a}_1 = L^{(f\Phi)}\Phi = 0$. Since any unit vector $\mathbf{u} \in R^n$ can be represented as a linear combination of $\{\mathbf{a}_j : j=1,...,n\}$, we can conclude that

$$|L^{(f\Phi)}\mathbf{u}| = O(f^{-1}v^{1/2}\kappa^{1/2}\zeta^{1/2}N_c^{1/2}) \tag{77}$$

It is shown later that $|L^{(ff)}| = O(f^{-2}\zeta^{-1}N_c)$ (see (94)) and $|\mathbf{u}^T L^{(\Phi\Phi)}\mathbf{u}| = O(v^{-1}\zeta^{-1}N_c)$ (see (85)). Combining these orders, we conclude

$$q_{f\Phi} = \max_{\substack{\mathbf{u}\in R^n \\ \|\mathbf{u}\|=1}} \frac{L^{(f\Phi)}\mathbf{u}}{[L^{(ff)}]^{1/2}[\mathbf{u}^T L^{(\Phi\Phi)}\mathbf{u}]^{1/2}} = O(v\kappa^{1/2}\zeta^{3/2}N_c^{-1/2}) << 1 \tag{78}$$

Similar arguments can be used to show that the cross-sensitivity of Φ with ζ or S is also small, whose details can be found in Appendix IV:

$$q_{\zeta\Phi} = O(v\zeta^{3/2}N_c^{-1/2}) << 1 \tag{79}$$

$$q_{S\Phi} = O(v\kappa\zeta^{3/2}N_c^{-1/2}) << 1 \tag{80}$$

Note also that $q_{S_e\Phi} = O(v^2\kappa^3\zeta^{7/2}n^{-1/2}N_c^{-1/2}) << 1$, as found before in (65).

6.2. Posterior covariance matrix

Since Φ is asymptotically decoupled from the remaining parameters its posterior covariance matrix is simply equal to the inverse of $L^{(\Phi\Phi)}$ in (31). Again, let $\{\mathbf{a}_j \in R^n : j=1,...,n\}$ be an orthonormal basis with $\mathbf{a}_1 = \Phi$. Using the asymptotic form of $\mathbf{A}_0$ in (48) and λ_0 in (49),

$$\lambda_0\mathbf{I}_n - \mathbf{A}_0 = \lambda_0\sum_{j=1}^n \mathbf{a}_j\mathbf{a}_j^T - [\lambda_0\mathbf{a}_1\mathbf{a}_1^T + S_eN_f\sum_{j=2}^n \mathbf{a}_j\mathbf{a}_j^T] = (\sum_k SD_k)\sum_{j=2}^n \mathbf{a}_j\mathbf{a}_j^T \tag{81}$$

Consequently,

$$L^{(\Phi\Phi)} \sim (2S_e^{-1}\sum_k SD_k)\sum_{j=2}^n \mathbf{a}_j\mathbf{a}_j^T = (2\sum_k \gamma_k)\sum_{j=2}^n \mathbf{a}_j\mathbf{a}_j^T \tag{82}$$

This indicates that $L^{(\Phi\Phi)}$ has a zero eigenvalue with eigenvector Φ. The remaining $(n-1)$ eigenvalues are $2\sum_k \gamma_k$, corresponding to the eigenvectors $\{\mathbf{a}_j : j=2,...,n\}$. This

is consistent with the fact that the NLLF is invariant to the scaling of $\boldsymbol{\Phi}$. In reality the mode shape is identified unambiguously with a norm constraint. It has been shown that when inverting $L^{(\Phi\Phi)}$ to obtain the covariance matrix the singularity along the direction $\boldsymbol{\Phi}$ can be ignored [23]. Consequently, the posterior covariance matrix of the mode shape is given by

$$\mathbf{C}_{\Phi} \sim (2\sum_k \gamma_k)^{-1} \sum_{j=2}^{n} \mathbf{a}_j \mathbf{a}_j^T = (2\sum_k \gamma_k)^{-1}(\mathbf{I}_n - \boldsymbol{\Phi}\boldsymbol{\Phi}^T) \tag{83}$$

Note that

$$2\sum_k \gamma_k = 2S_e^{-1}S\sum_k D_k \sim v^{-1}\zeta^{-1}N_c \tan^{-1}\kappa \tag{84}$$

since $\sum_k D_k = (N_c/2\zeta)\tan^{-1}\kappa$ from Table 3. Thus

$$L^{(\Phi\Phi)} \sim \frac{N_c \tan^{-1}\kappa}{v\zeta}(\mathbf{I}_n - \boldsymbol{\Phi}\boldsymbol{\Phi}^T) \tag{85}$$

$$\mathbf{C}_{\Phi} \sim \frac{v\zeta}{N_c \tan^{-1}\kappa}(\mathbf{I}_n - \boldsymbol{\Phi}\boldsymbol{\Phi}^T) \tag{86}$$

6.3. Expected MAC

Analogous to the deterministic case it has been shown that the posterior uncertainty of mode shape can be assessed by the expected value of the modal assurance criterion (MAC), i.e., cosine of the hyper-angle between the most probable mode shape and a random mode shape with the posterior distribution [23]. It can be shown that the expected MAC is given by

$$\bar{\rho} \sim (1+\sum_{j=2}^{n}\delta_j^2)^{-1/2} \tag{87}$$

where $\{\delta_j^2 : j = 1,...,n\}$ are the eigenvalues of $\mathbf{C}_{\Phi}$ arranged in ascending order of magnitude; $\delta_1 = 0$ as discussed before. This expression is asymptotically correct for $\delta_j \to 0$ ($j = 2,...,n$) or $n \to \infty$. Equation (86) implies that

$$\delta_j^2 \sim \frac{v\zeta}{N_c \tan^{-1}\kappa} \qquad j = 2,...,n \tag{88}$$

and so

$$\bar{\rho} \sim \left[1 + \delta_\Phi^2\right]^{-1/2} \tag{89}$$

where δ_Φ^2 is the sum of eigenvalues of $\mathbf{C}_\Phi$:

$$\delta_\Phi^2 = \sum_{j=2}^{n} \delta_j^2 \sim \frac{(n-1)v\zeta}{N_c \tan^{-1}\kappa} \tag{90}$$

Since $\bar{\rho}$ is often close to unity, it is more convenient to discuss based on δ_Φ^2. Note that $\bar{\rho} \sim 1 - \delta_\Phi^2/2 \sim \cos\delta_\Phi$ for small δ_Φ, and so δ_Φ can be interpreted as the equivalent mean hyper-angle between the uncertain mode shape and its MPV. Thus, δ_Φ is proportional to the overall uncertainty of mode shape.

7. Uncertainty law for frequency, damping and modal force PSD

The asymptotic decoupling of S_e and $\mathbf{\Phi}$ from the remaining parameters means that the posterior covariance matrix for f, ζ and S can be obtained from the inverse of the corresponding 3-by-3 partition of the Hessian. We shall next investigate the asymptotic behavior of this Hessian and its cross-sensitivities.

7.1. Auto-derivatives and cross-sensitivities

We first consider $L^{(ff)}$, recalling from (27). Using (116), the first term is given by

$$\sum_k (\ln D_k)^{(ff)} = 16f^{-2} \sum_k D_k^2 \beta_k^4 (\beta_k^2 - 1 + 2\zeta^2)^2 - 4f^{-2} \sum_k D_k \beta_k^2 (3\beta_k^2 - 1 + 2\zeta^2)$$

$$\sim 64f^{-2} \sum_k D_k^2 (\beta_k - 1)^2 - 8f^{-2} \sum_k D_k \tag{91}$$

On the other hand, using (111) from Appendix I, the second term in (27) is given by

$$S^{-1} \sum_k (D_k^{-1})^{(ff)} (\mathbf{\Phi}^T \mathbf{D}_k \mathbf{\Phi} + S_e) = 4S^{-1}f^{-2} \sum_k \beta_k^2 (3\beta_k^2 - 1 + 2\zeta^2)(\mathbf{\Phi}^T \mathbf{D}_k \mathbf{\Phi} + S_e)$$

$$\sim 8S^{-1}f^{-2} \sum_k (\mathbf{\Phi}^T \mathbf{D}_k \mathbf{\Phi} + S_e) \tag{92}$$

$$\sim 8f^{-2} \sum_k D_k$$

after using (50) and keeping the leading order terms. Combining (91) and (92) gives

$$L^{(ff)} \sim 64f^{-2} \sum_k D_k^2 (\beta_k - 1)^2 \tag{93}$$

Using Table 3 for the sum, we obtain

$$L^{(ff)} \sim \frac{4N_c}{f^2\zeta}(\tan^{-1}\kappa - \frac{\kappa}{\kappa^2+1}) \tag{94}$$

The asymptotic behavior of other derivatives $L^{(\zeta\zeta)}$, $L^{(f\zeta)}$, $L^{(\zeta S)}$ and $L^{(fS)}$ have been derived similarly in Appendix IV. The results are:

$$L^{(\zeta\zeta)} \sim \frac{4N_c}{\zeta}(\tan^{-1}\kappa + \frac{\kappa}{\kappa^2+1}) \tag{95}$$

$$L^{(f\zeta)} \sim -N_c f^{-1}\left[10\tan^{-1}\kappa - \frac{\kappa(22\kappa^2+18)}{(\kappa^2+1)^2}\right] \tag{96}$$

$$L^{(\zeta S)} \sim -4N_c S^{-1}\tan^{-1}\kappa \tag{97}$$

$$L^{(fS)} \sim N_c S^{-1}f^{-1}\zeta(4\kappa - 5\tan^{-1}\kappa + \frac{\kappa}{\kappa^2+1}) \tag{98}$$

We next assess the order of magnitude of the cross-sensitivities among f, ζ and S. The following can be deduced:

$$L^{(ff)} \sim O(f^{-2}\zeta^{-1}N_c),\ L^{(\zeta\zeta)} \sim O(\zeta^{-1}N_c),\ L^{(SS)} \sim O(S^{-2}\kappa\zeta N_c) \tag{99}$$

$$L^{(f\zeta)} \sim O(f^{-1}N_c),\ L^{(\zeta S)} \sim O(S^{-1}N_c),\ L^{(fS)} \sim O(S^{-1}f^{-1}\kappa\zeta N_c) \tag{100}$$

Based on the definition in (51), and using (99) and (100), it can be deduced that

$$q_{f\zeta} = O(\zeta),\ q_{\zeta S} = O(\kappa^{-1/2}),\ q_{fS} = O(\kappa^{1/2}\zeta) \tag{101}$$

7.2. Posterior variance

The posterior variances of f, ζ, S are given by the diagonals of the inverse of the corresponding 3-by-3 Hessian. Writing this Hessian in terms of the cross-sensitivity coefficients and taking matrix inverse gives, for the posterior variance of f,

$$\sigma_f^2 = L^{(ff)-1}(1-q_{\zeta S}^2)(1-q_{f\zeta}^2-q_{\zeta S}^2-q_{fS}^2+2q_{f\zeta}q_{\zeta S}q_{fS})^{-1} \tag{102}$$

The variance of ζ and S can be obtained analogously by rotating the roles of the variables. This expression can be further simplified by noting that

$$q_{\zeta S}^2 \gg q_{f\zeta}^2, q_{fS}^2, q_{f\zeta}q_{\zeta S}q_{fS} \tag{103}$$

which can be deduced from (101). As a result, the followings can be obtained:

$$\sigma_f^2 \sim L^{(ff)^{-1}}, \ \sigma_\zeta^2 \sim L^{(\zeta\zeta)^{-1}}(1-q_{\zeta S}^2)^{-1}, \ \sigma_S^2 \sim L^{(SS)^{-1}}(1-q_{\zeta S}^2)^{-1} \tag{104}$$

where $q_{\zeta S}^2$ is given by

$$q_{\zeta S}^2 = 2(\tan^{-1}\kappa)^2 \kappa^{-1}(\tan^{-1}\kappa + \frac{\kappa}{\kappa^2+1})^{-1} \tag{105}$$

Substituting (94), (135) (from Appendix IV) and (29) into (104), and using the definitions of c.o.v. (e.g., $\delta_f^2 = \sigma_f^2 / f^2$) gives the posterior c.o.v.s in (15).

7.3. Posterior correlation

The posterior correlation can be obtained as the off-diagonal terms of the posterior covariance matrix normalized by the square root product of the corresponding diagonals. This gives, between f and ζ,

$$\rho_{f\zeta} = \frac{q_{f\zeta} - q_{fS}q_{\zeta S}}{(1-q_{fS}^2)^{1/2}(1-q_{\zeta S}^2)^{1/2}} \tag{106}$$

The expressions for $\rho_{\zeta S}$ and ρ_{fS} can be obtained analogously by rotating the roles of the variables. Substituting the expressions of $q_{f\zeta}$, $q_{\zeta S}$ and q_{fS} leads to lengthy expressions for the correlations, which are omitted here as they carry limited insights. Nevertheless, in terms of scaling order, it can be deduced that

$$\rho_{f\zeta} = O(\zeta), \ \rho_{\zeta S} = O(\kappa^{-1/2}), \ \rho_{fS} = O(\kappa^{1/2}\zeta) \tag{107}$$

This indicates that, similar to the cross-sensitivity coefficients,

$$\rho_{\zeta S} \gg \rho_{f\zeta}, \rho_{fS} \tag{108}$$

8. Conclusions

Despite the lengthy mathematical derivations, the leading order behavior of the posterior variance of modal parameters is *remarkably simple*. The results are summarized in Table 1. They are asymptotically correct for small ζ and large N_c, N_f. As is common in asymptotic analysis, although the results are derived based on the asymptotic conditions, they can often give a good approximation in typical (non-asymptotic) situations. The

uncertainty laws have important implications on the extent to which one can reduce uncertainty and planning for ambient vibration tests. These shall be discussed in the companion paper, where the uncertainty laws shall also be verified using field data.

The frequency domain identification method adopted here does not introduce any loss of generality in the uncertainty laws because the posterior distribution (and hence its implied uncertainty) is unique for given modeling assumptions and data. Non-Bayesian methods tend to result in higher uncertainty (in a frequentist sense) because they may not have made use of all information contained in the data for inference.

It must be emphasized that our objective is not to use the uncertainty laws for actually calculating the posterior uncertainties given the data, since this can be done more accurately and in more general situations using the exact algorithms with little computational time. Rather, the scaling laws are derived to yield insights into the fundamental characteristics of the ambient modal identification problem. Mathematics is essential for a rigorous treatment, but it has never been the driving force directing this research. In fact the final results were conjectured qualitatively in the study of typhoon data [24], long before the mathematics was worked out.

9. Acknowledgements

10. References

[1] M.I. Friswell, J.E. Mottershead, Finite Element Model Updating in Structural Dynamics, Kluwer Academic Publishers, Dordrecht, 1995.

[2] S.W. Doebling, C.R. Farrar, M.B. Prime, D.W. Shevitz, A review of damage identification methods that examine changes in dynamic properties, Shock and Vibration Digest, 30 (2) (1998) 91–105.

[3] D.J. Ewins, Modal testing: Theory and Practice. Research Studies Press, PA, USA, 2000.

[4] F. Casciati, An overview of structural health monitoring expertise within the European Union, In: Wu ZS, Abe M, editors. Structural health monitoring and intelligent infrastructure. Lisse: Balkema; 2003. p. 31–7.

[5] B. Peeters, G. De Roeck, Stochastic system identification for operational modal analysis: a review, Journal of Dynamical Systems, Measurement, and Control, 123 (2001) 659-667.

[6] R. Brincker, L. Zhang, P. Anderson, Modal identification of output-only systems using frequency domain decomposition, Smart Materials and Structures, 10 (3) (2001) 441-455.

[7] J.M.W. Brownjohn, Ambient vibration studies for system identification of tall buildings, Earthquake Engineering and Structural Dynamics, 32 (2003) 71-95.

[8] S.K. Au, Fast Bayesian ambient modal identification in the frequency domain, Part I: posterior most probable value, Mechanical Systems and Signal Processing, 26 (1) (2012) 60-75.

[9] S. Alampalli, Significance of operating environment in condition monitoring of large civil structures, Shock and Vibration, 6(5–6) (1999) 247–51.

[10] J.M. Ko, J.Y. Wang, Y.Q. Ni, K.K. Chak, Observation on environmental variability of modal properties of a cable-stayed bridge from one-year monitoring data, In: Chang FK, editor. Structural health monitoring: from diagnostics and prognostics to structural health management. Lancaster (PA): DEStech. p. 467–74, 2003.

[11] J.T. Kim, C.B. Yun, J.H. Yi, Temperature effects on modal properties and damage detection in plate-girder bridges, In: Chang FK, Yun CB, Spencer Jr BF, editors. Advanced smart materials and structures technology. Lancaster (PA): DEStech; 504–511, 2004.

[12] S.K. Au, Y.C. Ni, F.L. Zhang, H.F. Lam, Full scale dynamic testing of a coupled slab system, Engineering Structures, 37 (2012) 167-178.

[13]   S.K. Au, Connecting Bayesian and frequentist quantification of parameter uncertainty in system Identification, Mechanical Systems and Signal Processing, 29 (2012) 328-342.

[14]   R.T. Cox, R. T., The Algebra of Probable Inference, Johns Hopkins, Baltimore, 1961.

[15]   E.T. Jaynes, Probability Theory: The Logic of Science. Cambridge University Press, UK, 2003.

[16]   J.L. Beck, Bayesian system identification based on probability logic, Structural Control and Health Monitoring, 17 (7) (2010) 825–847.

[17]   C. Papadimitriou, J.L. Beck, L.S. Katafygiotis, Updating robust reliability using structural test data, Probabilistic Engineering Mechanics, 16 (2) (2001) 103-113.

[18]   K.V. Yuen and L.S. Katafygiotis, Bayesian Fast Fourier Transform approach for modal updating using ambient data, Advances in Structural Engineering, 6 (2) (2003) 81-95.

[19]   S.K. Au, Fast Bayesian FFT method for ambient modal identification with separated modes, Journal of Engineering Mechanics, ASCE, 137 (3) (2011) 214-226.

[20]   S.K. Au, Fast Bayesian ambient modal identification in the frequency domain, Part II: posterior uncertainty, Mechanical Systems and Signal Processing, 26 (1) (2012) 76-90.

[21]   S. K. Au, F. L. Zhang and Y. C. Ni, Bayesian operational modal analysis: theory, computation, practice, Computers and Structures, (2013). In print. http://dx.doi.org/10.1016/j.compstruc.2012.12.015.

[22]   J. Schoukens, R. Pintelon, Identification of Linear Systems: A Practical Guideline for Accurate Modeling, Pergamon Press, London, 1991.

[23]   S.K. Au, F.L. Zhang, On assessing posterior mode shape uncertainty in ambient modal identification, Probabilistic Engineering Mechanics, 26 (3) (2011) 427-434.

[24]   S.K. Au, F.L. Zhang, P. To, Field observations on modal properties of two tall buildings in Hong Kong, Wind Engineering and Industrial Aerodynamics, 101 (2012) 12-23.

Appendix I. Derivatives of dynamic factor

This appendix presents the expressions for the derivatives of D_k, which are recalled from [19]. To simplify notations we put a parenthesized variable in the superscript to denote a derivative with respect to it. E.g., $D_k^{(f\zeta)}$ denotes $\partial^2 D_k / \partial f \partial \zeta$.

$\underline{D_k^{-1}}$

$$(D_k^{-1})^{(f)} = 4f^{-1}\beta_k^2(\beta_k^2 - 1 + 2\zeta^2) \tag{109}$$

$$(D_k^{-1})^{(\zeta)} = 8\zeta\beta_k^{\ 2} \tag{110}$$

$$(D_k^{-1})^{(ff)} = 4f^{-2}\beta_k^2(3\beta_k^{\ 2} - 1 + 2\zeta^2) \tag{111}$$

$$(D_k^{-1})^{(\zeta\zeta)} = 8\beta_k^{\ 2} \tag{112}$$

$$(D_k^{-1})^{(f\zeta)} = 16f^{-1}\zeta\beta_k^2 \tag{113}$$

$\underline{\ln D_k}$

$$(\ln D_k)^{(f)} = -4f^{-1}D_k\beta_k^2(\beta_k^2 - 1 + 2\zeta^2) \tag{114}$$

$$(\ln D_k)^{(\zeta)} = -8\zeta\beta_k^{\ 2}D_k \tag{115}$$

$$(\ln D_k)^{(ff)} = 16f^{-2}D_k^2\beta_k^4(\beta_k^2 - 1 + 2\zeta^2)^2 - 4f^{-2}D_k\beta_k^2(3\beta_k^2 - 1 + 2\zeta^2) \tag{116}$$

$$(\ln D_k)^{(\zeta\zeta)} = 8\beta_k^2 D_k(8\zeta^2\beta_k^2 D_k - 1) \tag{117}$$

$$(\ln D_k)^{(f\zeta)} = 16f^{-1}\zeta D_k^2\beta_k^2(\beta_k^4 - 1) \tag{118}$$

Appendix II. Asymptotics of discrete sums

This appendix investigates the asymptotic behavior of discrete sums of the form

$\sum_k D_k^a (\beta_k - 1)^b$, where a and b are integers and $b \geq 0$. The strategy is to express it as a Riemann sum and then approximate by an integral. This will be asymptotically correct when the number of terms N_f in the sum is large.

Recall from (7) that $D_k = [(\beta_k^2 - 1)^2 + (2\zeta\beta_k)^2]^{-1}$, where $\beta_k = f / f_k$. Note that $\{\beta_k\}$ are not evenly spaced, i.e., $\beta_{k+1} - \beta_k$ is not a constant of k. In order to write as a Riemann sum we shall define and work with an evenly spaced (dimensionless) coordinate. Let

$$u_k = \frac{f_k}{f} - 1 = \frac{1}{\beta_k} - 1 \tag{119}$$

By construction, $\{u_k\}$ are evenly spaced at $\Delta u = u_{k+1} - u_k = \Delta f / f$ where $\Delta f = T_d^{-1}$ and T_d is the data duration. Since $f = T^{-1}$ where T is the natural period, we have $\Delta u = T_d^{-1} / T^{-1} = N_c^{-1}$, where $N_c = T_d / T$. The lower and upper limit of u_k are $-\kappa\zeta$ and $+\kappa\zeta$, respectively.

Substituting $\beta_k = 1/(1 + u_k)$ into (7) and rearranging gives

$$D_k = \frac{(1 + u_k)^4}{u_k^2 (2 + u_k)^2 + 4\zeta^2 (1 + u_k)^2} \tag{120}$$

Using this form and noting that $\beta_k - 1 = -u_k / (1 + u_k)$, one obtains

$$\sum_k D_k^a (\beta_k - 1)^b = (-1)^b 2^{-2a} \sum_k \frac{(1 + u_k)^{4a-b} u_k^b}{[u_k^2 (1 + u_k / 2)^2 + \zeta^2 (1 + u_k)^2]^a} \tag{121}$$

Introducing $\Delta u = N_c^{-1}$ and approximating the Riemann sum by an integral, we have

$$\sum_k D_k^a (\beta_k - 1)^b \sim (-1)^b 2^{-2a} N_c \int_{-\kappa\zeta}^{\kappa\zeta} \frac{(1 + u)^{4a-b} u^b}{[u^2 (1 + u / 2)^2 + \zeta^2 (1 + u)^2]^a} du \tag{122}$$

Changing integration variable from u to u / ζ removes the dependence of the integration limit on ζ:

$$\sum_k D_k^a (\beta_k - 1)^b \sim (-1)^b 2^{-2a} N_c \zeta^{b-2a+1} \int_{-\kappa}^{\kappa} \frac{(1+\zeta u)^{4a-b} u^b}{[u^2 (1+\zeta u/2)^2 + (1+\zeta u)^2]^a} du \qquad (123)$$

The asymptotic approximation of this integral for small ζ is investigated in Appendix III. Based on this, asymptotic expressions for the discrete sums used in this work are derived and summarized in Table 3. Figure 1 compares the approximation with the exact values for the sums that are used in this work. It has been assumed that $f = 2\text{Hz}$ and $\zeta = 1\%$, although the plots for other values are similar. For each line, since ζ and N_c are fixed, $N_f = 2\zeta\kappa N_c$ is directly proportional to κ. For reference, N_f increases from 4 to 80 as κ increases from 1 to 20.

Scaling order

In terms of order of magnitude, it can be deduced that (see Appendix III) when b is even,

$$\sum_k D_k^a (\beta_k - 1)^b = \begin{cases} O(\kappa^{b-2a+1}\zeta^{b-2a+1}N_c) & \text{if} \quad b-2a+1>0 \\ O[(\log\kappa)\zeta^{b-2a+1}N_c] & \text{if} \quad b-2a+1=0 \\ O(\zeta^{b-2a+1}N_c) & \text{if} \quad b-2a+1<0 \end{cases} \qquad (124)$$

When b is odd,

$$\sum_k D_k^a (\beta_k - 1)^b = \begin{cases} O(\kappa^{b-2a+1+J_{ab}}\zeta^{b-2a+2}N_c) & \text{if} \quad b-2a+1+J_{ab}>0 \\ O[(\log\kappa)\zeta^{b-2a+2}N_c] & \text{if} \quad b-2a+1+J_{ab}=0 \\ O(\zeta^{b-2a+2}N_c) & \text{if} \quad b-2a+1+J_{ab}<0 \end{cases} \qquad (125)$$

where $J_{ab} = -1$ if $3a = b$ and $J_{ab} = 1$ otherwise. Comparing (124) and (125), when b is odd the sum is one order ζ less than its counterpart when b is even.

Appendix III. Asymptotics of integral (123)

This appendix investigates the asymptotics of the integral in (123) where a and b are integers and $b \geq 0$. For small ζ the absolute value of the integrand is roughly symmetric about the origin. When b is even the integrals on the positive and negative side tend to reinforce each other; when b is odd they tend to cancel out. The strategy is to use Taylor approximation with respect to ζ to capture the difference between the positive and negative part. Such difference is unimportant when b is even but it becomes the leading order when b is odd.

Let I_{ab} denote the integral in (123). Separate it into two parts, one on $[0, \kappa]$ and the other on $[-\kappa, 0]$. For the latter, change integration variable from u to $-u$. This gives

$$I_{ab} = \int_0^\kappa \frac{(1+\zeta u)^{4a-b} u^b}{[u^2(1+\zeta u/2)^2 + (1+\zeta u)^2]^a} + \frac{(1-\zeta u)^{4a-b} u^b (-1)^b}{[u^2(1-\zeta u/2)^2 + (1-\zeta u)^2]^a} du \tag{126}$$

The two integrands mainly differ by terms involving $\pm \zeta$. For small ζ,

$$\frac{(1 \pm \zeta u)^{4a-b} u^b}{[u^2(1 \pm \zeta u/2)^2 + (1 \pm \zeta u)^2]^a}$$

$$\sim \frac{u^b}{(1+u^2)^a} \left\{ 1 \pm \frac{\zeta u}{1+u^2}[(2a-b) + (3a-b)u^2] \right\} \tag{127}$$

When b is even the $O(\zeta)$ terms of the two integrands in (126) cancel out, giving

$$I_{ab} \sim 2 \int_0^\kappa \frac{u^b}{(1+u^2)^a} du \tag{128}$$

When b is odd, the zero-th order terms cancel out, leaving the $O(\zeta)$ terms as the leading order

$$I_{ab} \sim 2\zeta \int_0^\kappa \frac{u^{b+1}}{(u^2+1)^{a+1}}[(2a-b) + (3a-b)u^2] du \tag{129}$$

The integrals appearing in (128) and (129) can be evaluated analytically. Table 3 shows the resulting approximation of the discrete sum in (123) for $a = 1, 2$ and $b = 1, 2$ where the indefinite integrals that have been used are shown in the first column.

Scaling order

The scaling of I_{ab} with ζ is trivial. To investigate the scaling with κ, first consider the case when $b \geq 0$ is even. For large u, $u^b(1+u^2)^{-a} \sim u^{b-2a}$. This means that if $b-2a \leq -2$ then $\int_0^\kappa u^b(1+u^2)^{-a}\,du$ is bounded. Otherwise, it is asymptotic to $\int_0^\kappa u^{b-2a}\,du$ for large κ. Based on these, the following can be deduced when $b \geq 0$ is even:

$$I_{ab} = \begin{cases} O(\kappa^{b-2a+1}) & \text{if} \quad b-2a+1>0 \\ O(\log \kappa) & \text{if} \quad b-2a+1=0 \\ O(1) & \text{if} \quad b-2a+1<0 \end{cases} \tag{130}$$

The behavior for I_{ab} when $b \geq 0$ is odd can be similarly deduced:

$$I_{ab} = \begin{cases} O(\zeta \kappa^{b-2a+1+J_{ab}}) & \text{if} \quad b-2a+1+J_{ab}>0 \\ O(\zeta \log \kappa) & \text{if} \quad b-2a+1+J_{ab}=0 \\ O(\zeta) & \text{if} \quad b-2a+1+J_{ab}<0 \end{cases} \tag{131}$$

where $J_{ab} = -1$ if $3a=b$ and $J_{ab} = 1$ otherwise.

Appendix IV. Asymptotics of NLLF derivatives

This appendix derives the asymptotic expressions for those derivatives of the NLLF not covered in the main text. Cross sensitivities involving $\mathbf{\Phi}$ are also derived.

$\underline{L^{(\zeta\zeta)}}$

Recall $L^{(\zeta\zeta)}$ from (28). Using (117), the first term is given by

$$\sum_k (\ln D_k)^{(\zeta\zeta)} = 64\zeta^2 \sum_k \beta_k^4 D_k^2 - 8\sum_k \beta_k^2 D_k \sim 64\zeta^2 \sum_k D_k^2 - 8\sum_k D_k \tag{132}$$

Using (112), the second term in (28) is given by

$$S^{-1}\sum_k (D_k^{-1})^{(\zeta\zeta)}(\mathbf{\Phi}^T \mathbf{D}_k \mathbf{\Phi} + S_e) = 8S^{-1}\sum_k \beta_k^2 (\mathbf{\Phi}^T \mathbf{D}_k \mathbf{\Phi} + S_e)$$

$$\sim 8S^{-1}\sum_k (\mathbf{\Phi}^T \mathbf{D}_k \mathbf{\Phi} + S_e) \tag{133}$$

$$\sim 8\sum_k D_k$$

after using (50). Combining these two terms gives

$$L^{(\zeta\zeta)} \sim 64\zeta^2 \sum_k D_k^2 \tag{134}$$

Using Table 3 for the sum,

$$L^{(\zeta\zeta)} \sim \frac{4N_c}{\zeta}(\tan^{-1}\kappa + \frac{\kappa}{\kappa^2 + 1}) \tag{135}$$

$\underline{L^{(f\zeta)}}$

Recall $L^{(f\zeta)}$ from (32). Using (118), the first term is given by

$$\sum_k (\ln D_k)^{(f\zeta)} = 16f^{-1}\zeta \sum_k D_k^2 \beta_k^2 (\beta_k^4 - 1) \sim 64f^{-1}\zeta \sum_k D_k^{\ 2}(\beta_k - 1) \tag{136}$$

Using Table 3 for the sum,

$$\sum_k (\ln D_k)^{(f\zeta)} \sim -N_c f^{-1}\left[18\tan^{-1}\kappa - \frac{\kappa(22\kappa^2 + 18)}{(\kappa^2 + 1)^2}\right] \tag{137}$$

Using (113), the second term in (32) becomes

$$S^{-1} \sum_k (D_k^{-1})^{(f\zeta)} (\mathbf{\Phi}^T \mathbf{D}_k \mathbf{\Phi} + S_e)$$

$$= 16 S^{-1} f^{-1} \zeta \sum_k \beta_k^2 (\mathbf{\Phi}^T \mathbf{D}_k \mathbf{\Phi} + S_e)$$

$$\sim 16 S^{-1} f^{-1} \zeta \sum_k (\mathbf{\Phi}^T \mathbf{D}_k \mathbf{\Phi} + S_e) \qquad (138)$$

$$\sim 16 f^{-1} \zeta \sum_k D_k$$

after using (50). Using Table 3 for the sum,

$$S^{-1} \sum_k (D_k^{-1})^{(f\zeta)} (\mathbf{\Phi}^T \mathbf{D}_k \mathbf{\Phi} + S_e) \sim 8 N_c f^{-1} \tan^{-1} \kappa \qquad (139)$$

Combining (137) and (139),

$$L^{(f\zeta)} \sim -N_c f^{-1} \left[10 \tan^{-1} \kappa - \frac{\kappa(22\kappa^2 + 18)}{(\kappa^2 + 1)^2} \right] \qquad (140)$$

$\underline{L^{(\zeta S)}}$

Recall $L^{(\zeta S)}$ from (34). Using (110),

$$L^{(\zeta S)} = -8 S^{-2} \zeta \sum_k \beta_k^2 (\mathbf{\Phi}^T \mathbf{D}_k \mathbf{\Phi} + S_e)$$

$$\sim -8 S^{-2} \zeta \sum_k (\mathbf{\Phi}^T \mathbf{D}_k \mathbf{\Phi} + S_e) \qquad (141)$$

$$\sim -8 S^{-1} \zeta \sum_k D_k$$

after using (50). Using Table 3 for the sum

$$L^{(\zeta S)} = -4 N_c S^{-1} \tan^{-1} \kappa \qquad (142)$$

$\underline{L^{(fS)}}$

Substituting (109) into (33) gives

$$L^{(fS)} = -4 S^{-2} f^{-1} \sum_k \beta_k^2 (\beta_k^2 - 1 + 2\zeta^2)(\mathbf{\Phi}^T \mathbf{D}_k \mathbf{\Phi} + S_e)$$

$$\sim -8 S^{-2} f^{-1} \sum_k (\beta_k - 1)(\mathbf{\Phi}^T \mathbf{D}_k \mathbf{\Phi} + S_e) \qquad (143)$$

$$\sim -8 S^{-1} f^{-1} \sum_k D_k (\beta_k - 1)$$

after using (50). Using Table 3 for the sum,

$$L^{(fS)} \sim 2N_c S^{-1} f^{-1} \zeta (4\kappa - 5\tan^{-1}\kappa + \frac{\kappa}{\kappa^2+1}) \tag{144}$$

In the following we also assess the order of magnitude of the cross-sensitivities involving $\boldsymbol{\Phi}$. The technique is similar to that used in Section 6.1. As before $\{\mathbf{a}_j \in R^n : j = 1,...,n\}$ denotes an orthonormal basis with $\mathbf{a}_1 = \boldsymbol{\Phi}$.

$L^{(\zeta\Phi)}$ **and** $q_{\zeta\Phi}$

Using (40), for $j = 2,...,n$, since $\boldsymbol{\Phi}^T \mathbf{a}_j = 0$,

$$L^{(\zeta\Phi)}\mathbf{a}_j = 2S^{-1}\sum_k (D_k^{-1})^{(\zeta)}\boldsymbol{\Phi}^T \mathbf{D}_k \mathbf{a}_j = 2S^{-1}\sum_k (D_k^{-1})^{(\zeta)}(\boldsymbol{\Phi}^T \mathbf{F}_k \mathbf{F}_k^T \mathbf{a}_j + \boldsymbol{\Phi}^T \mathbf{G}_k \mathbf{G}_k^T \mathbf{a}_j) \tag{145}$$

Since $\mathbf{F}_k$ and $\mathbf{G}_k$ are i.i.d. it is sufficient to study the term related to $\mathbf{F}_k$. Using (110) and (70), and noting $v = S_e / S$,

$$2S^{-1}\sum_k (D_k^{-1})^{(\zeta)}\boldsymbol{\Phi}^T \mathbf{F}_k \mathbf{F}_k^{\ T}\mathbf{a}_j \sim 8v\zeta \sum_k \beta_k^2 \gamma_k^{1/2}(\mathbf{W}_k^T \mathbf{a}_j) X_k \tag{146}$$

Since $\mathbf{W}_k$ and X_k are uncorrelated this expression has zero mean. Its magnitude is then assessed by its standard deviation. Taking variance on both sides and taking $\beta_k^4 \sim 1$, $\mathbf{W}_k^T \mathbf{a}_j = 1$ and $E[X_k^2] = 1$, we have

$$\text{var}[2S^{-1}\sum_k (D_k^{-1})^{(\zeta)}\boldsymbol{\Phi}^T \mathbf{F}_k \mathbf{F}_k^T \mathbf{a}_j] \sim 64v\zeta^2 \sum_k D_k \tag{147}$$

Using (124) with $a = 1, b = 0$ (third case), $\sum_k D_k = O(\zeta^{-1}N_c)$ and so

$$\text{var}[2S^{-1}\sum_k (D_k^{-1})^{(\zeta)}\boldsymbol{\Phi}^T \mathbf{F}_k \mathbf{F}_k^{\ T}\mathbf{a}_j] = O(v\zeta N_c) \tag{148}$$

This means,

$$L^{(\zeta\Phi)}\mathbf{a}_j = O(v^{1/2}\zeta^{1/2}N_c^{1/2}) \qquad\qquad j = 2,...,n \tag{149}$$

Together with the fact that $L^{(\zeta\Phi)}\mathbf{a}_1 = L^{(\zeta\Phi)}\boldsymbol{\Phi} = 0$, we obtain, for any unit vector $\mathbf{u} \in R^n$,

$$L^{(\zeta\Phi)}\mathbf{u} = O(v^{1/2}\zeta^{1/2}N_c^{1/2}) \tag{150}$$

Combining with $|L^{(\zeta\zeta)}| = O(\zeta^{-1}N_c)$ (see (135)) and $|\mathbf{u}^T L^{(\Phi\Phi)}\mathbf{u}| = O(v^{-1}\zeta^{-1}N_c)$ (see (85)), we conclude

$$q_{\zeta\Phi} = \max_{\substack{\mathbf{u} \in R^n \\ \|\mathbf{u}\|=1}} \frac{L^{(\zeta\Phi)}\mathbf{u}}{[L^{(\zeta\zeta)}]^{1/2}[\mathbf{u}^T L^{(\Phi\Phi)}\mathbf{u}]^{1/2}} = O(\nu\zeta^{3/2}N_c^{-1/2}) << 1 \tag{151}$$

$\underline{L^{(S\Phi)}}$ **and** $\underline{q_{S\Phi}}$

Using (41), for $j = 2,...,n$,

$$L^{(S\Phi)}\mathbf{a}_j \sim -2S^{-2}\sum_k D_k^{-1}\mathbf{\Phi}^T\mathbf{D}_k\mathbf{a}_j = -2S^{-2}\sum_k D_k^{-1}(\mathbf{\Phi}^T\mathbf{F}_k\mathbf{F}_k^T\mathbf{a}_j + \mathbf{\Phi}^T\mathbf{G}_k\mathbf{G}_k^T\mathbf{a}_j) \tag{152}$$

Using (70),

$$2S^{-2}\sum_k D_k^{-1}\mathbf{\Phi}^T\mathbf{F}_k\mathbf{F}_k^T\mathbf{a}_j \sim \nu^{1/2}S^{-1}\sum_k D_k^{-1/2}(\mathbf{W}_k^T\mathbf{a}_j)X_k \tag{153}$$

Again, we assess the order of magnitude of this expression by its standard deviation:

$$\mathrm{var}[2S^{-2}\sum_k D_k^{-1}\mathbf{\Phi}^T\mathbf{F}_k\mathbf{F}_k^T\mathbf{a}_j] \sim \nu S^{-2}\sum_k D_k^{-1} \tag{154}$$

Using (124) with $a = -1, b = 0$ (first case), $\sum_k D_k^{-1} = O(\kappa^3\zeta^3 N_c)$ and so

$$\mathrm{var}[2S^{-2}\sum_k D_k^{-1}\mathbf{\Phi}^T\mathbf{F}_k\mathbf{F}_k^T\mathbf{a}_j] = O(\nu S^{-2}\kappa^3\zeta^3 N_c) \tag{155}$$

$$L^{(S\Phi)}\mathbf{a}_j = O(\nu^{1/2}S^{-1}\kappa^{3/2}\zeta^{3/2}N_c^{1/2}) \qquad j = 2,3,...,n \tag{156}$$

Thus, for any unit vector $\mathbf{u} \in R^n$,

$$L^{(S\Phi)}\mathbf{u} = O(\nu^{1/2}S^{-1}\kappa^{3/2}\zeta^{3/2}N_c^{1/2}) \tag{157}$$

Combining with $|L^{(SS)}| = O(S^{-2}\kappa\zeta N_c)$ (see (29)) and $|\mathbf{u}^T L^{(\Phi\Phi)}\mathbf{u}| = O(\nu^{-1}\zeta^{-1}N_c)$ (see (85)),

$$q_{S\Phi} = O(\nu\kappa\zeta^{3/2}N_c^{-1/2}) << 1 \tag{158}$$

$\underline{L^{(S_e\Phi)}}$ **and** $\underline{q_{S_e\Phi}}$

Recall $L^{(S_e\Phi)}$ from (63). For $j = 2,...,n$,

$$L^{(S_e\Phi)}\mathbf{a}_j \sim -2S^{-2}\sum_k D_k^{-2}\mathbf{\Phi}^T\mathbf{D}_k\mathbf{a}_j = -2S^{-2}\sum_k D_k^{-2}(\mathbf{\Phi}^T\mathbf{F}_k\mathbf{F}_k^T\mathbf{a}_j + \mathbf{\Phi}^T\mathbf{G}_k\mathbf{G}_k^T\mathbf{a}_j) \tag{159}$$

Using (70),

$$-2S^{-2}\sum_k D_k^{-2}\mathbf{\Phi}^T\mathbf{F}_k\mathbf{F}_k^T\mathbf{a}_j \sim -S_e S^{-2}\sum_k D_k^{-2}\gamma_k^{1/2}(\mathbf{W}_k^T\mathbf{a}_j)X_k \tag{160}$$

The order of magnitude of this expression is assessed by its standard deviation:

$$\text{var}[-2S^{-2}\sum_k D_k^{-2}\mathbf{\Phi}^T\mathbf{F}_k\mathbf{F}_k^T\mathbf{a}_j] \sim v^3 S_e^{-2}\sum_k D_k^{-3} \tag{161}$$

Using (124) with $a=-3, b=0$ (first case), $\sum_k D_k^{-3} = O(\kappa^7\zeta^7 N_c)$ and so

$$\text{var}[2S^{-2}\sum_k D_k^{-2}\mathbf{\Phi}^T\mathbf{F}_k\mathbf{F}_k^T\mathbf{a}_j] = O(v^3 S_e^{-2}\kappa^7\zeta^7 N_c) \tag{162}$$

$$L^{(S_e\Phi)}\mathbf{a}_j = O(v^{3/2}S_e^{-1}\kappa^{7/2}\zeta^{7/2}N_c^{1/2}) \tag{163}$$

Thus, for any unit vector $\mathbf{u} \in R^n$,

$$L^{(S_e\Phi)}\mathbf{u} = O(v^{3/2}S_e^{-1}\kappa^{7/2}\zeta^{7/2}N_c^{1/2}) \tag{164}$$

Combining with $|L^{(S_eS_e)}| = O(S_e^{-2}\kappa\zeta n N_c)$ (see (30)) and $|\mathbf{u}^T L^{(\Phi\Phi)}\mathbf{u}| = O(v^{-1}\zeta^{-1}N_c)$ (see (85)),

$$q_{S_e\Phi} = O(v^2\kappa^3\zeta^{7/2}n^{-1/2}N_c^{-1/2}) << 1 \tag{165}$$

List of Tables
Table 1. Summary of posterior uncertainty law. Variance on diagonals; correlation on off-diagonals
Table 2. Summary of sensitivity coefficients
Table 3. Summary of approximation for discrete sums

List of Figures
Figure 1. Approximation of discrete sums. f =2Hz, ζ =1%. Circle: exact; line: approximate

Table 1. Summary of posterior uncertainty law. Variance on diagonals; correlation on off-diagonals

	f	ζ	S	S_e	$\mathbf{\Phi}$
f	$\dfrac{f^2\zeta}{4N_c}(\tan^{-1}\kappa - \dfrac{\kappa}{\kappa^2+1})^{-1}$				
ζ	$O(\zeta)$	$\dfrac{\zeta}{4N_c}\left[\tan^{-1}\kappa + \dfrac{\kappa}{\kappa^2+1} - \dfrac{2(\tan^{-1}\kappa)^2}{\kappa}\right]^{-1}$		Sym.	
S	$O(\kappa^{1/2}\zeta)$	$O(\kappa^{-1/2})$	$\dfrac{S^2}{N_f}\left[1 - \dfrac{2(\tan^{-1}\kappa)^2}{\kappa(\tan^{-1}\kappa + \dfrac{\kappa}{\kappa^2+1})}\right]^{-1}$		
S_e	$O(\nu\kappa^{5/2}\zeta^3 n^{-1/2})$	$O(\nu\kappa^{3/2}\zeta^2 n^{-1/2})$	$O(\nu\kappa^2\zeta^2 n^{-1/2})$	$\dfrac{S_e^2}{(n-1)N_f}$	
$\mathbf{\Phi}$	$O(\nu\kappa^{1/2}\zeta^{3/2}N_c^{-1/2})$	$O(\nu\kappa^{1/2}\zeta^{3/2}n^{-1/2}N_c^{-1/2})$	$O(\nu\kappa\zeta^{3/2}N_c^{-1/2})$	$O(\nu^2\kappa^3\zeta^{7/2}n^{-1/2}N_c^{-1/2})$	$\dfrac{\nu\zeta}{N_c\tan^{-1}\kappa}(\mathbf{I}_n - \mathbf{\Phi}\mathbf{\Phi}^T)$

Table 2. Summary of sensitivity coefficients

	f	ζ	S	S_e	Φ
f	1				
ζ	$O(\zeta)$	1		Sym.	
S	$O(\kappa^{1/2}\zeta)$	$O(\kappa^{-1/2})$	1		
S_e	$O(\nu\kappa^{5/2}\zeta^3 n^{-1/2})$	$O(\nu\kappa^{1/2}\zeta^2 n^{-1/2})$	$O(\nu\kappa^2\zeta^2 n^{-1/2})$	1	
Φ	$O(\nu\kappa^{1/2}\zeta^{3/2}N_c^{-1/2})$	$O(\nu\zeta^{3/2}n^{-1/2}N_c^{-1/2})$	$O(\nu\kappa\zeta^{3/2}N_c^{-1/2})$	$O(\nu^2\kappa^3\zeta^{7/2}n^{-1/2}N_c^{-1/2})$	1

Table 3. Summary of approximation for discrete sums

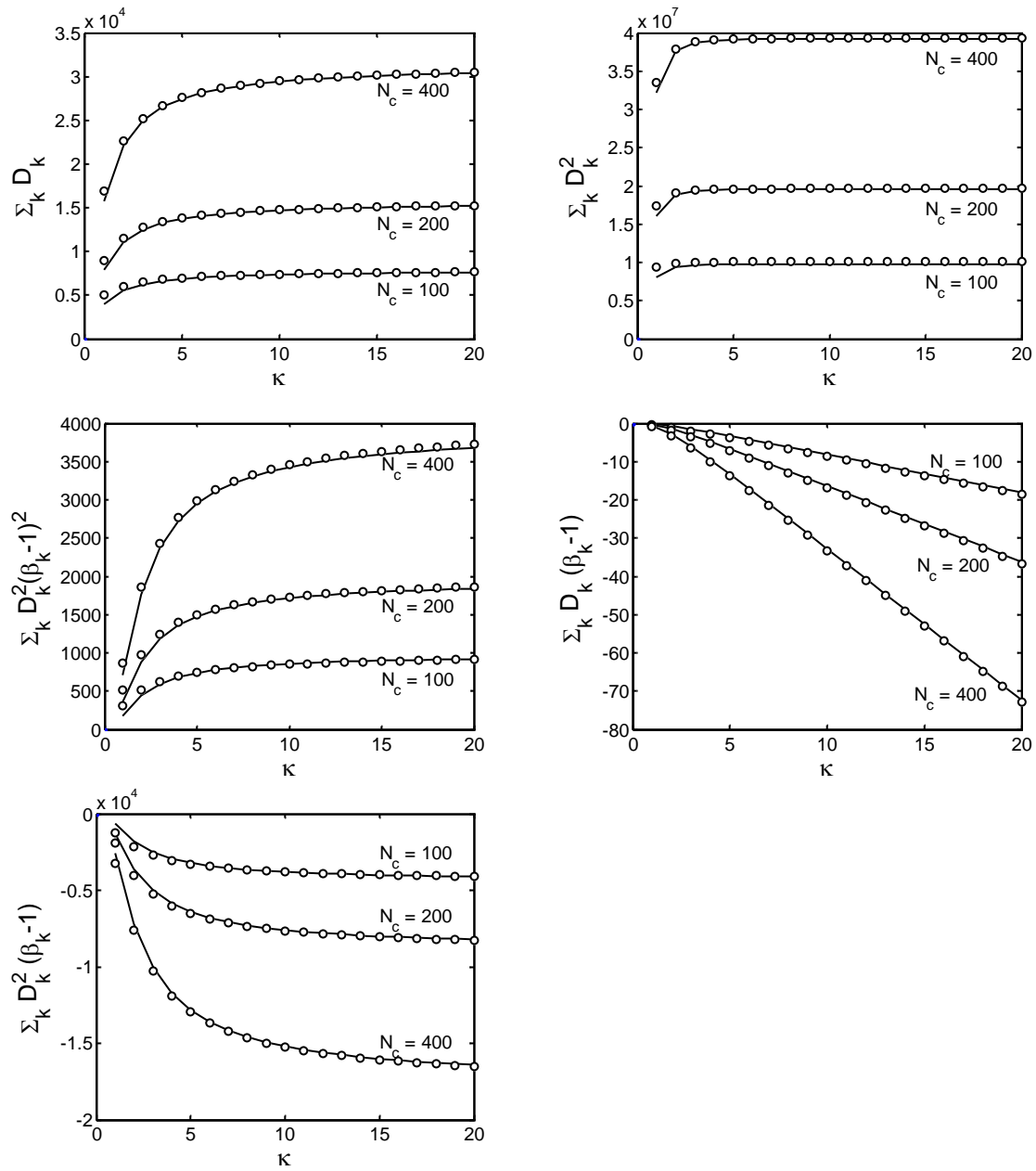| Integral	Sum
$\displaystyle \int \frac{du}{u^2+1} = \tan^{-1} u$	$\displaystyle \sum_k D_k \sim \frac{N_c}{2\zeta}\tan^{-1}\kappa$
$\displaystyle \int \frac{du}{(u^2+1)^2} = \frac{1}{2}(\tan^{-1} u + \frac{u}{u^2+1})$	$\displaystyle \sum_k D_k^2 \sim \frac{N_c}{16\zeta^3}(\tan^{-1}\kappa + \frac{\kappa}{\kappa^2+1})$
$\displaystyle \int \frac{u^2 du}{(u^2+1)^2} = \frac{1}{2}(\tan^{-1} u - \frac{u}{u^2+1})$	$\displaystyle \sum_k D_k^2(\beta_k-1)^2 \sim \frac{N_c}{16\zeta}(\tan^{-1}\kappa - \frac{\kappa}{\kappa^2+1})$
$\displaystyle \int \frac{u^4 du}{(u^2+1)^2} = \frac{1}{2}(2u - 3\tan^{-1} u + \frac{u}{u^2+1})$	$\displaystyle \sum_k D_k(\beta_k-1) \sim -\frac{N_c\zeta}{4}(4\kappa - 5\tan^{-1}\kappa + \frac{\kappa}{\kappa^2+1})$
$\displaystyle \int \frac{u^2 du}{(u^2+1)^3} = \frac{1}{8}\left[\tan^{-1} u + \frac{u(u^2-1)}{(u^2+1)^2}\right]$	$\displaystyle \sum_k D_k^2(\beta_k-1) \sim -\frac{N_c}{32\zeta}\left[9\tan^{-1}\kappa - \frac{\kappa(11\kappa^2+9)}{(\kappa^2+1)^2}\right]$
$\displaystyle \int \frac{u^4 du}{(u^2+1)^3} = \frac{1}{8}\left[3\tan^{-1} u - \frac{u(5u^2+3)}{(u^2+1)^2}\right]$	

Figure 1. Approximation of discrete sums. f =2Hz, ζ =1%. **Circle: exact; line: approximate**